*Int. J. Solids Structures*, 1975, Vol. 11, pp. 1057–1078. Pergamon Press. Printed in Gt. Britain.

# CYLINDRICAL ELASTIC-PLASTIC WAVES DUE TO DISCONTINUOUS LOADING AT A CIRCULAR CAVITY

M. G. SRINIVASAN†

Argonne National Laboratories, Argonne, IL 60439, U.S.A.

and

T. C. T. TING‡

Materials Engineering Department, University of Illinois at Chicago Circle, Chicago, IL 60680, U.S.A.

(*Received* 25 *October* 1974; *revised* 24 *February* 1975)

**Abstract**—The plastic waves in rate-independent, isotropically work-hardening media obeying the von Mises yield condition generated by radial stress uniformly applied at a circular cavity of radius $r = r_0$, are studied. Both plane stress and plane strain motions are considered. The radial stress and its time derivative at the cavity may be discontinuous at time $t = t_0$. If the applied radial stress is continuous while its time derivative is not, the discontinuity at $(r_0, t_0)$ propagates into $r > r_0$ along the characteristics and/or the elastic-plastic boundaries. If the applied radial stress itself is discontinuous, the discontinuity in stress may propagate into $r > r_0$ in the form of a shock wave, or a pseudo centered simple wave, or a combination of both. This is a systematic study on the nature of solutions in the neighborhood of $(r_0, t_0)$ for all possible combinations of discontinuous loadings applied at $(r_0, t_0)$. The special cases of linear work-hardening and perfectly-plastic media are also discussed. Finally, the corresponding problem for materials obeying the Tresca yield condition is studied briefly.

## 1. INTRODUCTION

It appears that very little has been done on axisymmetric cylindrical waves in a thin plate or in an infinite medium of elastic, isotropically work-hardening material due to an applied radial stress at a circular cavity; although the corresponding problem for specialized materials such as elastic, and elastic perfectly-plastic media have been studied.

For waves in a thin plate in which the stress state can be considered as plane stress, Kromm [1], Plass and Ellis [2], and Chou and Koenig [3] studied the case when the plate is elastic. Cristescu [4] derived the expressions for plastic wave speeds in a thin plate using three different constitutive relations. He considered the general case in which the shear stress $\sigma_{r\theta}$ is non-zero but did not discuss the solutions of the governing equations.

For radial waves in a thick walled tube of infinite length in which the state of strain is plane strain, Agababian [5] studied the case when the material is perfectly-plastic and obeys the Tresca yield condition. The authors's assumption of elastic incompressibility greatly simplifies the problem, and makes it possible to derive an ordinary differential equation for the position of the loading boundary. In another paper [6], he considered the same problem without assuming elastic incompressibility. He used a total deformation theory and assumed that the maximum shear stress is equal to $(\sigma_{\theta\theta} - \sigma_{rr})/2$. Bronskii [7] obtained a closed form solution for the velocity of the inner surface of a thick-walled tube subjected to an internal gas pressure. The material is assumed to be incompressible and elastic, perfectly-plastic, satisfying the Tresca yield condition. Stepanenko [8] studied the same problem assuming that the inner surface was given a uniformly distributed impulse. Cristescu [9] derived the characteristic wave speeds for the cylindrical waves in elastic, perfectly-plastic materials. Again, he considered the general case $\sigma_{r\theta} \neq 0$, but did not discuss the solutions of the governing equations.

From the experimental point of view, it is clear that there are technical difficulties in generating plane stress waves in a thin plate. By contrast, plane strain waves in a hollow cylinder are relatively simpler to obtain as can be seen from numerous published results. For example, Ensminger and Fyfe [10] devised an experiment aimed at the evaluation of constitutive models. Their experimental technique involved the generation of plane strain plastic waves propagating

†Assistant Mechanical Engineer.
‡Professor of Applied Mechanics.

radially from the center of a hollow cylindrical specimen. Fyfe[11] made a comparison between the experimental results and the theoretical predictions of a rate-independent plasticity theory for an aluminum alloy. This theory is based on a generalized form of the Koehler–Seitz bilinear model. The plastic wave speed is constant and the solution is obtained by a numerical integration along the straight line characteristics. The theoretical predictions did not agree well with the experimental results; and an elastic, viscoplastic theory was used in a subsequent paper[12]. It was concluded that while certain forms of rate-dependent theory predict the experimental results for certain ranges of stress and strain rate, the elastic, viscoplastic model is not necessarily the only possible model. More discussions on rate effects in plastic wave propagation can be found in recent works by Malvern[13] and Clifton[14]. Finally, we mention the paper by Duffey[15] in which the transient response of a uniformly expanding, impulsively loaded, thin-walled cylinder is obtained for an elastic, perfectly-plastic material. Because of the assumption that $\sigma_{rr} = 0$ and that the change in the wall thickness is negligible, the problem is simplified.

For an elastic material, a unified theory such as the one by Chou and Koenig[3] can be used to treat plane stress waves and plane strain waves simultaneously. Unfortunately, this is not possible for elastic-plastic materials unless a drastic assumption is made, such as the one made by Mehta[16] who assumed that $\sigma_{zz} = \epsilon_{zz} = 0$ for both plane stress and plane strain waves. Nevertheless, the results presented here show that, in most cases, a single expression can be used for both plane stress and plane strain solutions.

In this paper, we present the solutions of cylindrically symmetric waves near the inner circular boundary due to a uniformly distributed radial stress at the circular cavity. The applied radial stress can be continuous or discontinuous. The material is assumed to be rate-independent, elastic, isotropically work-hardening and obeying the von Mises yield condition. Basic equations for cylindrical waves of plane stress and plane strain are derived in Section 2. The solutions for plane stress waves are presented in Section 3. Since the analysis is similar to that of spherical waves[17], it is presented briefly here. It should be mentioned however that while the plastic wave speed is a function of the yield stress for the spherical waves, it is a function of all stress components for the cylindrical waves. The cases of plane strain waves are presented in Section 4. We see that most solutions in Section 3 can be used for Section 4 if the variables are redefined. In Section 5, the special cases of linear work-hardening and perfectly-plastic solids are discussed. Finally, plastic waves in solids obeying the Tresca yield condition are investigated in Section 6.

## 2. BASIC EQUATIONS FOR CYLINDRICAL WAVES

When the waves are cylindrically symmetric, the equation of motion is

$$\sigma_{rr,r} + (\sigma_{rr} - \sigma_{\theta\theta})/r = \rho\dot{v} \tag{2.1}$$

where $\sigma_{rr}$ and $\sigma_{\theta\theta}$ are the radial and circumferential stresses, $v$ is the radial particle velocity, $\rho$ is the mass density, $r$ is the radial distance. The comma and dot denote partial differentiation on $r$ and time $t$, respectively. If $\epsilon_{rr}$ and $\epsilon_{\theta\theta}$ are the radial and circumferential strains, the material continuity requires that

$$\dot{\epsilon}_{rr} = v_{,r}, \qquad \dot{\epsilon}_{\theta\theta} = v/r. \tag{2.2}$$

We will use the von Mises yield condition and the associated flow rule. Let

$$f = s_{ij}s_{ij}/2, \qquad s_{ij} = \sigma_{ij} - \delta_{ij}\sigma_{kk}/3 \tag{2.3}$$

where $\sigma_{ij}$ is the stress tensor. The plastic yield is reached if

$$f = k^2 \tag{2.4}$$

where $k > 0$ is the yield stress whose magnitude depends on the previous work-hardening history. The stress-strain relation for isotropic work-hardening materials can be written as (Hill[18]),

$$\dot{\epsilon}_{ij} = \frac{1+\nu}{E}\dot{\sigma}_{ij} - \frac{\nu}{E}\delta_{ij}\dot{\sigma}_{kk} + G\frac{\partial f}{\partial \sigma_{ij}}\frac{\partial f}{\partial \sigma_{pq}}\dot{\sigma}_{pq} \tag{2.5}$$

where $E$ is Young's modulus, $\nu$ is Poisson's ratio and $G > 0$ is a known function of $k$. $G = 0$ in the elastic region. By considering the special case of uniaxial stress-strain relation in which $\sigma$ and $\epsilon$ are the longitudinal stress and strain, respectively, eqn (2.5) is reduced to[19],

$$G(k) = \frac{3}{4k^2E}\left(\frac{1}{\beta(\sqrt{(3k)})} - 1\right) \tag{2.6}$$

where $\beta$ is a function of $\sqrt{(3k)}$ and is given by

$$\beta(\sigma) = \frac{1}{E}\frac{\mathrm{d}\sigma}{\mathrm{d}\epsilon} \tag{2.7}$$

In the elastic region $\beta = 0$; while in the plastic region $0 < \beta \leq 1$. In the plastic region, we assume that $\beta$ is a strictly decreasing function of $\sigma$, although the cases of linear work-hardening ($\beta$ = constant) and perfectly-plastic solids ($\beta = 0$) are discussed in Section 5.

## 3. PLANE STRESS WAVES

### 3.1 *Introduction*

For cylindrically symmetric waves in which a plane stress state exists, the only non-zero stresses are $\sigma_{rr}$ and $\sigma_{\theta\theta}$. For simplicity, we will write

$$p = \sigma_{rr}, \qquad q = \sigma_{\theta\theta}. \tag{3.1}$$

The yield function eqn (2.3) then becomes

$$f = \frac{1}{3}(p^2 + q^2 - pq) \tag{3.2}$$

and eqn (2.5) reduces to, after using eqns (2.2) and (2.6),

$$Ev_{,r} = \dot{p} - \nu\dot{q} + \frac{3}{4}\left(\frac{1}{\beta} - 1\right)s_r(s_r\dot{p} + s_\theta\dot{q})/k^2 \tag{3.3}$$

$$E\frac{v}{r} = -\nu\dot{p} + \dot{q} + \frac{3}{4}\left(\frac{1}{\beta} - 1\right)s_\theta(s_r\dot{p} + s_\theta\dot{q})/k^2 \tag{3.4}$$

where

$$s_r = \frac{1}{3}(2p - q), \qquad s_\theta = \frac{1}{3}(2q - p) \tag{3.5}$$

Equations (2.1), (3.3) and (3.4) can now be written in the form of the matrix differential equation

$$\mathbf{A}\dot{\mathbf{w}} + \mathbf{B}\mathbf{w}_{,r} = \frac{1}{r}\mathbf{F}\mathbf{w} \tag{3.6}$$

where

$$\mathbf{w} = \begin{bmatrix} v \\ p \\ q \end{bmatrix}, \quad \mathbf{A} = \begin{bmatrix} \rho & 0 & 0 \\ 0 & \frac{1}{E}\left\{1 + \frac{3}{4}s_r^2\left(\frac{1}{\beta} - 1\right)\Big/k^2\right\} & \frac{1}{E}\left\{-\nu + \frac{3}{4}s_rs_\theta\left(\frac{1}{\beta} - 1\right)\Big/k^2\right\} \\ 0 & \frac{1}{E}\left\{-\nu + \frac{3}{4}s_rs_\theta\left(\frac{1}{\beta} - 1\right)\Big/k^2\right\} & \frac{1}{E}\left\{1 + \frac{3}{4}s_\theta^2\left(\frac{1}{\beta} - 1\right)\Big/k^2\right\} \end{bmatrix} \tag{3.7}$$

$$B = \begin{bmatrix} 0 & -1 & 0 \\ -1 & 0 & 0 \\ 0 & 0 & 0 \end{bmatrix}, \qquad F = \begin{bmatrix} 0 & 1 & -1 \\ 0 & 0 & 0 \\ 1 & 0 & 0 \end{bmatrix}$$

The characteristic wave speeds $c$ of eqn (3.6) are the roots of

$$\|c\mathbf{A} - \mathbf{B}\| = 0 \tag{3.8}$$

which yields $c = 0, \pm c_p$ in the plastic region where

$$\frac{1}{c_p} = \frac{1}{c_L}\left\{1 + \frac{(1-\beta)s^2}{(1-\nu^2)[12\beta k^2 + (1-\beta)(p-2q)^2]}\right\}^{1/2} \tag{3.9}$$

$$c_L = \left\{\frac{E}{\rho(1-\nu^2)}\right\}^{1/2} \tag{3.10}$$

$$s = (2-\nu)p - (1-2\nu)q \tag{3.11}$$

In the elastic region $\beta = 1$ and the roots are $0, \pm c_L$. Notice that $c_p = c_L$ also when $s = 0$ regardless of the value of $\beta$.

The left eigenvector $\mathbf{l}$ and the right eigenvector $\mathbf{r}$, defined by

$$\mathbf{l}^T(c\mathbf{A} - \mathbf{B}) = \mathbf{0}, \qquad (c\mathbf{A} - \mathbf{B})\mathbf{r} = \mathbf{0}, \tag{3.12}$$

are identical for the present problem because $\mathbf{A}$ and $\mathbf{B}$ are both symmetric. For $c = c_L, c_p$, we have

$$\mathbf{r} = \begin{bmatrix} 1 \\ -\rho c \\ -\rho c\psi \end{bmatrix} \tag{3.13}$$

$$\psi(\beta) = \nu + \frac{(1-\beta)(p-2q)s}{12\beta f + (1-\beta)(p-2q)^2} \tag{3.14}$$

Notice that $\psi = \nu$ when $\beta = 1$, or $p = 2q$, or $s = 0$.

For $c \neq 0$, the total derivative of $\mathbf{w}$ along a characteristic is

$$\left.\frac{d\mathbf{w}}{dr}\right|_c \equiv \mathbf{w}_{,r} + \frac{1}{c}\dot{\mathbf{w}}, \qquad (c = c_L, c_p). \tag{3.15}$$

Elimination of $\mathbf{w}_{,r}$ between eqns (3.15) and (3.6) yields

$$(c\mathbf{A} - \mathbf{B})\dot{\mathbf{w}} = c\left(\frac{1}{r}\mathbf{F}\mathbf{w} - \mathbf{B}\left.\frac{d\mathbf{w}}{dr}\right|_c\right). \tag{3.16}$$

The characteristic condition is obtained by applying eqn (3.12$_1$):

$$\mathbf{r}^T\mathbf{B}\left.\frac{d\mathbf{w}}{dr}\right|_c = \frac{1}{r}\mathbf{r}^T\mathbf{F}\mathbf{w}. \tag{3.17}$$

If $\lambda$ is the speed of an elastic-plastic boundary, it was shown in [20] that

$$\frac{\dot{f}^p}{\dot{f}^e} = \frac{\|\lambda\mathbf{A}^e - \mathbf{B}\|}{\|\lambda\mathbf{A}^p - \mathbf{B}\|}, \tag{3.18}$$

where the superscripts $e$ and $p$ denote evaluation in the elastic and plastic regions, respectively.

We will write $\lambda = c_u$ for an unloading wave and $\lambda = c_l$ for a loading wave. If $\dot{f}^e$ and $\dot{f}^p$ are not both zero, it can be shown that[21, 22]

$$c_p \leq c_u \leq c_L, \qquad c_l \geq c_L \quad \text{or} \quad c_l \leq c_p. \tag{3.19}$$

3.2 *Continuous loading*

Consider a circular cavity of radius $r_0$ in an infinite medium which is subjected to a prescribed radial stress $p(r_0, t)$ at the cavity along with prescribed initial conditions, such as $p(r, 0)$, $q(r, 0)$, and $v(r, 0)$. Suppose that $p(r_0, t)$ is continuous with respect to $t$ except at $t = t_0$ when $p(r_0, t)$ or its time derivative $\dot{p}(r_0, t)$ may be discontinuous. We will study the nature of the solution in the neighborhood of $r = r_0$, $t = t_0$. In this section we consider the cases in which $p(r_0, t)$ is continuous while $\dot{p}(r_0, t)$ may be discontinuous at $t = t_0$. The cases in which both $p(r_0, t)$ and $\dot{p}(r_0, t)$ are discontinuous at $t = t_0$ will be considered in Section 3.3.

Without loss of generality we take $t_0 = 0$ and assume that the solution for $r \geq r_0$, $t \leq -0$ has been obtained. The discontinuity at $(r_0, 0)$ will in general propagate into the region $r > r_0$, $t > 0$ along more than one line and divide the neighborhood of $(r_0, 0)$ into several regions bounded by the lines of discontinuities (see Fig. 1). Each region will be denoted by $a$, $b$ or $m$, etc. with $a$ and $b$ reserved for the uppermost and lowermost regions, respectively. Any quantity with superscript $a$, $b$, $m$, ... stands for the limiting value of that quantity in that region with $(r, t)$ approaching $(r_0, 0)$. In particular

$$p^a = \lim_{t \to +0} p(r_0, t), \qquad p^b = \lim_{t \to -0} p(r_0, t), \tag{3.20}$$

and hence $p^a$ and $p^b$ are the values of $p(r_0, t)$ just "after" and "before" $t = 0$, respectively. Of course we are assuming that there is no line of discontinuities converging from $r > r_0$, $t < 0$ towards $(r_0, 0)$. In the present section, $p(r_0, t)$ is assumed to be continuous at $t = 0$. Consequently

$$p^a = p^b = p^m. \tag{3.21}$$

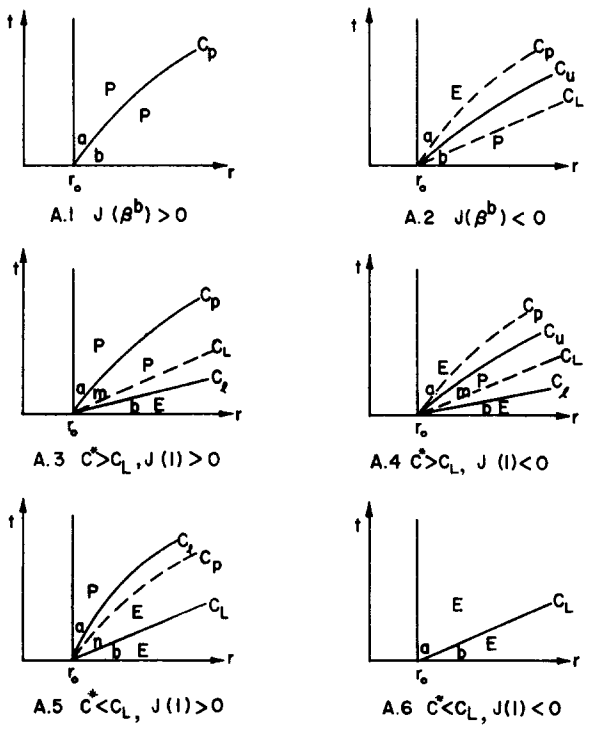


Fig. 1. $p^a = p^b$, and $f^b = k^{02}$. ($E$ and $P$ stand for "elastic" and "plastic" regions, respectively.)

We will also use the superscript 0 on quantities such as the speed of the elastic-plastic boundary to indicate the limiting value of that quantity at $(r_0, 0)$.

The solution in the neighborhood of $(r_0, 0)$ depends on the given values $\dot{p}^b$ and $\dot{p}^a$ as well as on whether the region $b$ is plastic or elastic. There are six possible cases as shown in Fig. 1. The analysis is similar to that of [17, 23] and hence is presented briefly here. The solid lines are the lines of discontinuity while the dotted lines are given in the figures for the purpose of showing the relative positions of the solid lines. There is no discontinuity across the dotted lines. $E$ and $P$ stand for elastic and plastic regions, respectively.

In all six cases, the radial stress $p$ is continuous. It can be shown by the conservation of momentum that the velocity $v$ is also continuous. By applying eqn (3.4) to both sides of a line of discontinuity $\Gamma$, we obtain

$$\left[\left\{\nu - \left(\frac{1}{\beta} - 1\right)\left(\frac{p^2 + q^2}{4k^2} - \frac{5}{4}\right)\right\}\dot{p}\right] = \left[\left\{1 + \left(\frac{1}{\beta} - 1\right)\left(1 - \frac{p^2}{4k^2}\right)\right\}\dot{q}\right] \tag{3.22}$$

where [*] stands for the difference in the values of * on the two sides of $\Gamma$. If $\Gamma$ is a characteristic both sides of $\Gamma$ will be in the same state (i.e. elastic, or plastic) and hence $\beta$ is the same on both sides. Equation (3.22) then can be written as

$$[\dot{q}] = [\dot{p}]\psi(\beta) \tag{3.23}$$

where $\psi(\beta)$ is defined in eqn (3.14).

It should be noticed that eqn (3.22) applies not only to two regions which are adjacent to each other. It also applies to two regions which are separated by another region such as regions $a$ and $b$ in Cases A.3, A.4 and A.5 of Fig. 1.

For Case A.1, the region $a$ is plastic. Hence $\dot{f}^a > 0$, or by eqn (3.2),

$$(2p^a - q^a)\dot{p}^a + (2q^a - p^a)\dot{q}^a > 0 \tag{3.24}$$

By applying eqn (3.23) to regions $a$ and $b$, and eliminating $\dot{q}^a$ from eqn (3.24), we obtain

$$J(\beta^b) > 0 \tag{3.25}$$

$$J(\beta^b) = s^b(\dot{p}^a - \dot{p}^b) + \dot{f}^b\left\{3 + \left(\frac{1}{\beta^b} - 1\right)(p^b - 2q^b)^2/(4f^b)\right\} \tag{3.26}$$

Therefore, if $\dot{p}^a$, $\dot{p}^b$ and $\dot{q}^b$ satisfy the condition (3.25), we have Case A.1.

For Case A.2, the region $a$ is elastic and we have

$$(2p^a - q^a)\dot{p}^a + (2q^a - p^a)\dot{q}^a < 0 \tag{3.27}$$

This reduces to the condition $J(\beta^b) < 0$ when $\dot{q}^a$ is obtained from eqn (3.22).

When the region $b$ is elastic, we have to consider the maximum yield stress $k^*(r)$ ever reached at each $r$ for $t < 0$. If the material has never been loaded into a plastic region for $t < 0$, $k^*(r)$ is a constant and is equal to the initial yield stress. Let

$$k^0 = k^*(r_0), \qquad k^0_{,r} = k^*_{,r}(r_0) \tag{3.28}$$

We will assume that

$$f^b = (p^{b^2} + q^{b^2} - p^b q^b)/3 = (k^0)^2, \tag{3.29}$$

i.e. the stress state at $(r_0, 0^-)$ has reached a yield stress. Otherwise the discontinuity will propagate along $r = r_0 + c_L t$ and the problem is trivial. The elastic solution in region $b$ can be extended up to the elastic characteristic $r = r_0 + c_L t$ provided the stress state remains elastic throughout. To see if we can extend the elastic solution all the way up to $r = r_0 + c_L t$, we consider the yield function $f$ along any line $r = r_0 + c^* t$. For small $(r - r_0)$, we have

$$f\left(r, \frac{r-r_0}{c^*}\right) = f^b + (f^b_{,r} + \dot{f}^b/c^*)(r-r_0) + 0\{(r-r_0)^2\}. \tag{3.30}$$

On the other hand,

$$k^{*2}(r) = k^{0^2} + 2k^0 k^0_{,r}(r-r_0) + 0\{(r-r_0)^2\}. \tag{3.31}$$

If the yield stress is reached along $r = r_0 + c^* t$, we should have

$$f^b_{,r} + \dot{f}^b/c^* = 2k^0 k^0_{,r} \tag{3.32}$$

or

$$c^* = \dot{f}^b/(2k^0 k^0_{,r} - f^b_{,r}) \tag{3.33}$$

Hence, if $c^* > c_L$, we have Cases A.3 and A.4. Otherwise, we have Cases A.5 and A.6. In Cases A.3 and A.5, eqns (3.22) and (3.24) apply which yield the condition $J(1) > 0$. $J(1)$ is the value of $J(\beta^b)$ defined in eqn (3.26) with $\beta^b = 1$. Similarly, for Cases A.4 and A.6, eqns (3.22) and (3.27) reduce to $J(1) < 0$.

As can be seen from Fig. 1 where the conditions to be applied to each case are indicated, the six cases are mutually exclusive. If the inequality condition which governs the case becomes an equality, we have to consider the higher-order derivatives and employ an analysis similar to that of [24] to determine which case the problem belongs to.

3.3 *Discontinuous loading*

In this section we will study the cases in which $p^a$ and $p^b$ are not equal. Thus, we have a strong discontinuity in $p(r, t)$ at $(r_0, 0)$. This strong discontinuity may propagate into the region $r > r_0$ as a shock wave or spread out into something like a centered simple wave with center at $(r_0, 0)$. To analyze the singular nature of the solution near $(r_0, 0)$, we use the procedure by Ting [25] and expand $\mathbf{w}$ in a power series in $t$:

$$\mathbf{w}(r, t) = \mathbf{w}^{(0)}(\lambda) + t\mathbf{w}^{(1)}(\lambda) + \cdots, \tag{3.34}$$

$$\lambda = (r - r_0)/t, \tag{3.35}$$

where $\mathbf{w}^{(0)}, \mathbf{w}^{(1)}, \ldots$ are functions of $\lambda$ only. If we substitute eqn (3.34) into eqn (3.6) and equate coefficients of terms of the like powers in $t$, we obtain the differential equations for $\mathbf{w}^{(0)}, \mathbf{w}^{(1)}, \ldots$ in a recurrence form. In particular, $\mathbf{w}^{(0)}$ is governed by

$$(\lambda \mathbf{A}^{(0)} - \mathbf{B}) \frac{d\mathbf{w}^{(0)}}{d\lambda} = 0, \qquad \mathbf{A}^{(0)} = \mathbf{A}(\mathbf{w}^{(0)}). \tag{3.36}$$

Let $c^{(0)}$ be the positive root of

$$\|c^{(0)}\mathbf{A}^{(0)} - \mathbf{B}\| = 0. \tag{3.37}$$

The solution of eqn ($3.36_1$) depends on whether $\lambda = c^{(0)}$ or not. We call a region "regular" if $\lambda \neq c^{(0)}$ and "singular" if $\lambda = c^{(0)}$.

In the regular region, it is seen that $\mathbf{w}^{(0)}$ is a constant vector.

In the singular region, $d\mathbf{w}^{(0)}/d\lambda$ is proportional to the right eigen-vector $\mathbf{r}$ given by eqn (3.13), and hence

$$\frac{dv}{1} = \frac{dp}{-\rho c} = \frac{dq}{-\rho c \psi} \tag{3.38}$$

in which the superscript (0) is omitted. The last equality gives

$$dq/dp = \psi. \tag{3.39}$$

Since $\psi$ as defined in eqn (3.14) is a known function of $p$ and $q$, eqn (3.39) can be integrated numerically once the function $\beta$ is specified. Integration of eqn (3.39) yields a one-parameter family of curves in the $p \sim q$ plane, Fig. 2. The ellipse is the yield surface given in eqn (3.2). The arrows show the direction along which $(p, q)$ vary as $\lambda$ decreases. Inside the yield surface the stress state can vary along either direction.

Although eqn (3.39) in general cannot be integrated analytically, the curves in Fig. 2 can be sketched fairly accurately if the following observations are made. $\psi$ in eqn (3.39) is the slope of the curves and, by eqn (3.14), $\psi = \nu$ when $\beta = 1$, or $p = 2q$, or $s = 0$. In Fig. 2 this means that the slope is equal to $\nu$ in the elastic region and along the lines MN and HD. The curves are symmetric with respect to the origin 0. $\psi = 0$ along the curve FGN which resembles a hyperbola with OF and ON the asymptotes and G the vertex. Point G corresponds to $p = q$ and $\beta = (1+4\nu)^{-1}$. $\psi < 0$ inside the curve FGN, $0 < \psi < \nu$ in the region HDFGNM, and $\psi > \nu$ in the region NMH'D'.

For linearly work-hardening ($\beta$ = constant) and ideally plastic solids ($\beta = 0$), eqn (3.39) can be integrated analytically. (See Section 5). If $\beta$ is an arbitrary function of $\sqrt{(3k)}$, eqn (3.39) can be integrated when $\nu = 1/2$. For, when $\nu = 1/2$ eqn (3·39) reduces to

$$\left(\frac{1}{\beta} - 1\right)\frac{dk}{k} = -\frac{d(p-2q)}{(p-2q)} \tag{3.40}$$

The solution $\mathbf{w}^{(0)}$ in the singular region resembles a simple wave solution and it would be a simple wave solution if the right-hand side of eqn (3.6) were zero. For this reason, we call $\mathbf{w}^{(0)}$ the psuedo-simple wave solution. The solutions for $\mathbf{w}^{(1)}$ in the singular region are not needed here.

### 3.4 *Propagation of shock waves*

If the discontinuous loading applied at $r = r_0$ is propagated into $r > r_0$ as a shock wave, the speed of the shock wave will be the elastic wave speed $c_L$ even if the stress states just behind and ahead of shock wave are plastic due to a sudden reversal in the loading. If we consider the discontinuity across the shock wave as the limit of a continuous variation over an infinitesimal interval, the state of stress within this interval is elastic. The discontinuity in $\mathbf{w}$ across the shock wave which is denoted by $[\mathbf{w}]$ therefore satisfies the relation

$$[\mathbf{w}] = \gamma \mathbf{r}^e, \tag{3.41}$$

where $\gamma$ is a proportional factor which depends on the distance along the shock wave. From this

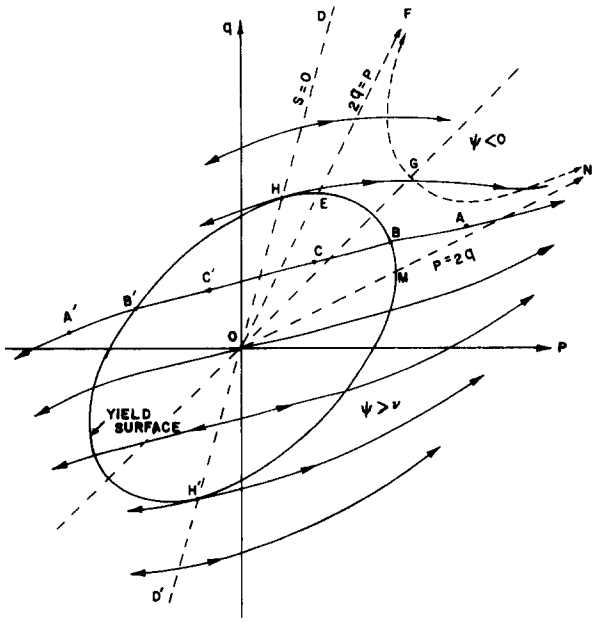


Fig. 2. Stress paths for pseudo-simple waves. (Plane stress and von Mises yield condition.)

and eqn (3.13), we have

$$3[f] = (\delta\rho c_L\gamma)^2 - s^-\rho c_L\gamma \tag{3.42}$$

$$3\left[\frac{df}{dr}\bigg|_{c_L}\right] = 2(\delta\rho c_L)^2\gamma\frac{d\gamma}{dr} - s^-\rho c_L\frac{d\gamma}{dr} - \rho c_L\gamma\frac{ds^-}{dr} \tag{3.43}$$

where

$$\delta = (1 - \nu + \nu^2)^{1/2} \tag{3.44}$$

Also from eqn (3.41)

$$\left[\frac{d\mathbf{w}}{dr}\bigg|_{c_L}\right] = \frac{d\gamma}{dr}\mathbf{r}^e, \qquad \mathbf{r}^{eT}\mathbf{B}\left[\frac{d\mathbf{w}}{dr}\bigg|_{c_L}\right] = \rho c_L\frac{d\gamma}{dr}. \tag{3.45}$$

Finally, we apply eqn (3.16) to both sides of a shock wave and subtract the results. We obtain, after using eqns (3.14) and ($3.45_1$),

$$[(c_L\mathbf{A} - \mathbf{B})\dot{\mathbf{w}}] = c_L\left\{\frac{1}{r}\gamma\mathbf{F} - \frac{d\gamma}{dr}\mathbf{B}\right\}\mathbf{r}^e \tag{3.46}$$

If we know $\gamma$ and $d\gamma/dr$, eqn (3.46) may be used to determine $\dot{\mathbf{w}}$ on one side of the shock wave if $\dot{\mathbf{w}}$ on the other side is known. The differential equation governing $\gamma$ has different forms depending on whether the region just before or after the shock is elastic or plastic. These cases are discussed separately as follows.

(i) *Elastic-elastic discontinuity.* If we apply eqn (3.17) to both sides of the shock wave and subtract the results, we obtain, after using eqns (3.41) and ($3.45_2$),

$$\frac{d\gamma}{dr} = -\frac{\gamma}{2r} \tag{3.47}$$

(ii) *Elastic-plastic discontinuity.* If we substitute $\mathbf{w}^e = \mathbf{w}^p + \gamma\mathbf{r}^e$ into eqn (3.17), we obtain,

$$\frac{d\gamma}{dr} + \frac{\gamma}{2r} = \frac{1}{2\rho c_L}\mathbf{r}^{eT}\left\{\frac{1}{r}\mathbf{F}\mathbf{w}^p - \mathbf{B}\frac{d\mathbf{w}^p}{dr}\bigg|_{c_L}\right\} \tag{3.48}$$

The right-hand side of eqn (3.48) can be expressed in terms of $\dot{p}^p$ and $\dot{q}^p$ by using eqn (3.16) and noticing that

$$\mathbf{r}^{eT}(c_L\mathbf{A}^p - \mathbf{B})\dot{\mathbf{w}}^p = c_L\mathbf{r}^{eT}(\mathbf{A}^p - \mathbf{A}^e)\dot{\mathbf{w}}^p. \tag{3.49}$$

Hence, eqn (3.48) can be written

$$\frac{d\gamma}{dr} + \frac{\gamma}{2r} + \frac{1}{8E}\left(\frac{1}{\beta} - 1\right)s^p\dot{f}^p/f^p = 0 \tag{3.50}$$

(iii) *Plastic-plastic discontinuity.* In this case, $f^+ = f^-$ and eqn (3.42) reduces to

$$\gamma = s^-/(\rho c_L\delta^2) \tag{3.51}$$

3.5 *Cases of discontinuous loadings*

We will divide the discontinuous loadings into several groups according to the relative positions of $(p^b, q^b)$ and $(p^a, q^a)$ on a stress path shown in Fig. 2. With the exception of Group I, each group has more than one case depending, among others, on the values of $\dot{p}^b$, $\dot{q}^b$ and $\dot{p}^a$. The values of $\dot{p}^b$, $\dot{q}^b$ and $\dot{p}^a$ are assumed to be given. If we apply eqn (3.4) to regions $a$ and $b$ and subtract the results, we obtain

$$\dot{f}^a\left\{3+\frac{1}{4f^a}\left(\frac{1}{\beta^a}-1\right)(2q^a-p^a)^2\right\}=\bar{J}(\beta^b) \tag{3.52}$$

where

$$\bar{J}(\beta^b)=s^a(\dot{p}^a-\dot{p}^b)+(2p^a-q^a)\dot{p}^b+(2q^a-p^a)\dot{q}^b + \left(\frac{1}{\beta^b}-1\right)(2q^b-p^b)(2q^a-p^a)\dot{f}^b/(4f^b)+(2q^a-p^a)E(v^a-v^b)/r_0 \tag{3.53}$$

and $v^a-v^b$ is, by eqn (3.38),

$$v^a-v^b=-\int_{p^b}^{p^a}\frac{\mathrm{d}p}{\rho c} \tag{3.54}$$

Since $(p, q)$ follows a stress path in Fig. 2, $c$ in eqn (3.54) depends on $p$ only. Equation (3.52) provides the solution for $\dot{q}^a$. Notice that $\bar{J}(\beta^b)$ reduces to $J(\beta^b)$ of eqn (3.26) when $p^a=p^b$.

If region $a$ is plastic, $\dot{f}^a>0$ and hence $\bar{J}(\beta^b)>0$ by eqn (3.52). This condition applied to Groups II, III and V. In contrast, $\bar{J}(\beta^b)<0$ applies when region $a$ is elastic in Groups II, III and V.

*Group I*

In this group, the stress state in both regions $a$ and $b$ is inside the yield surface. Hence,

$$f^b<k^{0^2}, \qquad f^a<k^{0^2} \tag{3.55}$$

The jump from $p^b$ to $p^a$ can be from point C to C′ or from C′ to C in Fig. 2. Since

$$q^a=q^b+\nu(p^a-p^b) \tag{3.56}$$

eqn ($3.55_2$) becomes

$$\delta^2(p^a-p^b)^2+s^b(p^a-p^b)+3(f^b-k^{0^2})<0 \tag{3.57}$$

or

$$|2\delta^2(p^a-p^b)+s^b|<\Delta \tag{3.58}$$

$$\Delta=\{s^{b^2}+12\delta^2(k^{0^2}-f^b)\}^{1/2} \tag{3.59}$$

Equation (3·58) gives the condition to be satisfied for this group in addition to eqn ($3.55_1$). The discontinuity is propagated along $c_L$, Fig. 3. The double lines stand for the shock wave. Equation (3.47) applies to this case which, upon integration, gives

$$\gamma=\gamma^0(r_0/r)^{1/2} \tag{3.60}$$

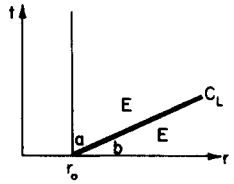


Fig. 3. Group I: $f^b<k^{0^2}$, $|2\delta^2(p^a-p^b)+s^b|<\Delta$. (Double lines stand for shock wave.)

where $\gamma^0$ is obtained by using eqn (3.42). Since $\gamma$ as given by eqn (3.60) does not vanish for finite $r$, the shock wave does not disappear at a finite distance.

*Group II*

In this group, the jump from $p^b$ to $p^a$ is from point C or C′ which is inside the yield surface to point A or A′ which is outside the yield surface in Fig. 2. Mathematically, this kind of discontinuity is expressed by eqn (3.55$_1$) and

$$|2\delta^2(p^a - p^b) + s^b| > \Delta. \tag{3.61}$$

There are four cases in this group and are shown in Fig. 4. S stands for the singular region which is always plastic. If the singular region is bounded from below and above by plastic characteristics, $c_p$ of course has different values at the upper boundary from those of the lower boundary. In all four cases, the stress state $(p^n, q^n)$ is equivalent to point B or B′ in Fig. 2. Hence,

$$2\delta^2(p^n - p^b) = \{sgn(p^a - p^b)\}\Delta - s^b \tag{3.62}$$

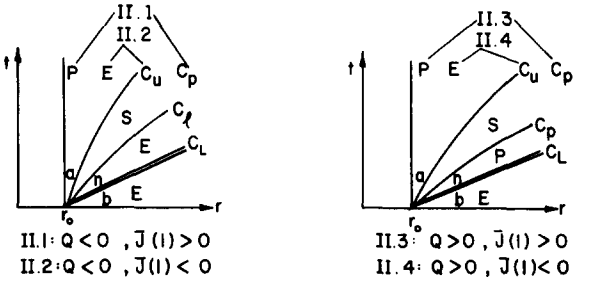


Fig. 4. Group II: $f^b < k^{0^2}$, $|2\delta^2(p^a - p^b) + s^b| > \Delta$. ($S$ stands for "singular" region.)

In Cases II.1 and II.2, the region $n$ is elastic. This means that

$$\left(\frac{df}{dr}\bigg|_{c_L}\right)^n < \frac{d}{dr}(k^0)^2 \tag{3.63}$$

It can be shown that (see [17]) this condition is equivalent to $Q < 0$ where

$$Q = 3\left\{\left(\frac{df}{dr}\bigg|_{c_L}\right)^b - \frac{d}{dr}(k^0)^2\right\} + (p^n - p^b)\left\{\left(\frac{ds}{dr}\bigg|_{c_L}\right)^b - \frac{s^b}{2r_0} - \frac{\delta^2}{r_0}(p^n - p^b)\right\} \tag{3.64}$$

Similarly, it can be shown that $Q > 0$ for Cases II.3 and II.4 when the region $n$ is plastic.

*Group III*

In this group, the jump from $p^b$ to $p^a$ is from point B (or B′) which is at a yield surface to point A (or A′) which is at a higher yield surface, Fig. 2. Mathematically, this is given by the following two conditions:

$$f^b = k^{0^2}, \qquad (p^a - p^b)/s^b > 0. \tag{3.65}$$

It is interesting to notice that if $(p^b, q^b)$ is at the point H in Fig. 2, then regardless of the value of $p^a$ the stress state $(p^a, q^a)$ will be at a higher yield surface. Hence, if $s^b = 0$, $p^a$ is arbitrary for Group III. The analysis of this group is omitted here but the results are shown in Fig. 5.

*Group IV*

In this group, the jump from $p^b$ to $p^a$ is either from point B to C or C′, or from point B′ to C or C′, Fig. 2. Mathematically, this is given by eqn (3.65$_1$) and

$$0 > (p^a - p^b)/s^b > -1/\delta^2 \tag{3.66}$$

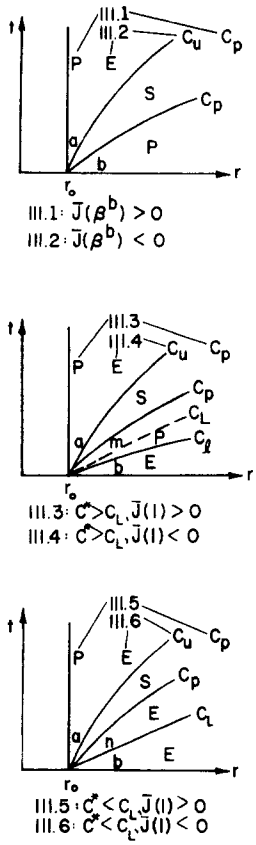


Fig. 5. Group III: $f^b = k^{02}$ and (i) $(p^a - p^b)/s^b > 0$, if $s^b \neq 0$, (ii) $p^a$ arbitrary, if $s^b = 0$.

If region $b$ is plastic, we have Case IV.1, Fig. 6. The propagation of shock wave is obtained by integrating eqn (3.50). Unlike the case of the elastic-elastic shock wave in Group I, the plastic-elastic shock wave in general disappears at a finite distance. If region $b$ is elastic, we have Cases IV.2 or IV.3 depending on whether $c^* \lesseqgtr c_L$.

*Group V*

In this group, the jump from $p^b$ to $p^a$ is either from point B to A′ or from point B′ to A, Fig. 2. This is expressed by eqn $(3.65_1)$ and

$$(p^a - p^b)/s^b < -1/\delta^2 \tag{3.67}$$

As shown in Fig. 7, there are twelve cases in this group. All singular regions in this group involve a "reversed plastic" loading. The region $n$ is characterized by the relation

$$\delta^2(p^n - p^b) + s^b = 0 \tag{3.68}$$

In Case V.1 and V.2, the region $n$ is elastic. This means that

$$\left(\frac{df}{dr}\bigg|_{c_L}\right)^n < \left(\frac{df}{dr}\bigg|_{c_L}\right)^b \tag{3.69}$$

It can be shown that this is equivalent to $R^b > 0$ where

$$R^b = \frac{1}{2r_0} + \frac{1}{s^b}\left(\frac{ds}{dr}\bigg|_{c_L}\right)^b + \frac{\rho\delta^2 c_L}{8E}\left(\frac{1}{\beta^b} - 1\right)\frac{\dot{f}^b}{f^p} \tag{3.70}$$

By a similar argument, $R^b < 0$ applies to Cases V.3 and V.4.

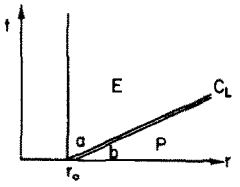


IV.1

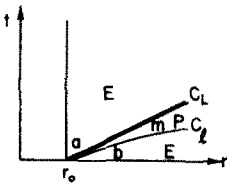


IV.2: $C^e > C_L$

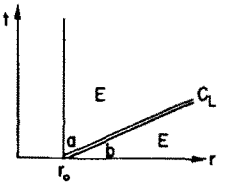


IV.3: $C^e < C_L$

Fig. 6. Group IV: $f^b = k^{02}, 0 > (p^a - p^b)/s^b > -1/\delta^2, s^b \neq 0$.

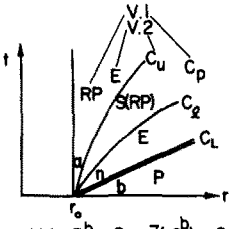


V.1: $R^b > 0$, $J(\beta^b) > 0$
V.2: $R^b > 0$, $J(\beta^b) < 0$

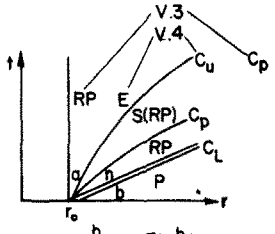


V.3: $R^b < 0$, $J(\beta^b) > 0$
V.4: $R^b < 0$, $J(\beta^b) < 0$

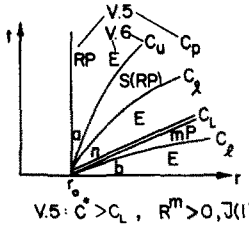


V.5: $C^e > C_L$, $R^m > 0$, $J(l) > 0$
V.6: $C^e > C_L$, $R^m > 0$, $J(l) < 0$

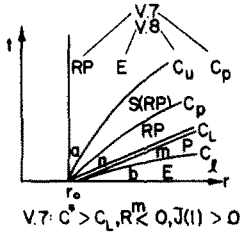


V.7: $C^e > C_L$, $R^m < 0$, $J(l) > 0$
V.8: $C^e > C_L$, $R^m < 0$, $J(l) < 0$

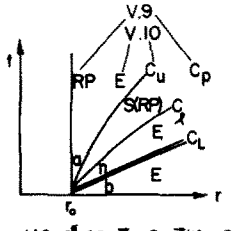


V.9: $C^e < C_L, \bar{Q} < 0$, $J(l) > 0$
V.10: $C^e < C_L, \bar{Q} < 0$, $J(l) < 0$

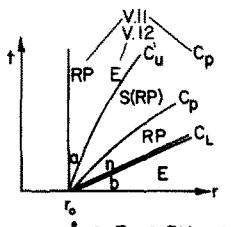


V.11: $C^e < C_L, \bar{Q} > 0$, $J(l) > 0$
V.12: $C^e < C_L, \bar{Q} > 0$, $J(l) < 0$

Fig. 7. Group V: $f^b = k^{02}, (p^a - p^b)/s^b < -1/\delta^2, s^b \neq 0$.

For Cases V.5 through V.8, the region $b$ is elastic and $c^* > c_L$. Hence $c^* = c_i^0$. If we ignore region $b$, Cases V.5–V.8 are identical to Cases V.1–V.4. Therefore, instead of the condition $R^b \gtrless 0$, we have the condition $R^m \gtrless 0$. To obtain $R^m$, $\dot{p}^m$ and $\dot{q}^m$ are determined from eqn (3.18) and (3.22) while $p^m_{,r}$ and $q^m_{,r}$ are determined by the continuity condition along $c^*$:

$$\dot{p}^m + c^* p^m_{,r} = \dot{p}^b + c^* p^b_{,r} \tag{3.71}$$

$$\dot{q}^m + c^* q^m_{,r} = \dot{q}^b + c^* q^b_{,r} \tag{3.72}$$

For Cases V.9–V.12, the region $b$ is elastic and $c^* < c_L$. These are actually special cases of Group II in which $(p^b, q^b)$ is at the yield surface. Hence, if we use eqn (3.68), we obtain the condition $\bar{Q} \gtrless 0$ where

$$\bar{Q} = 3\left\{\left(\frac{df}{dr}\bigg|_{c_L}\right)^b - \frac{d}{dr}(k^0)^2\right\} - \frac{s^b}{\delta^2}\left\{\left(\frac{ds}{dr}\bigg|_{c_L}\right)^b + \frac{s^b}{2r_0}\right\} \tag{3.73}$$

*Groups II′ and V′*

These are limiting cases of Groups II and V. In Group II, if

$$|2\delta^2(p^a - p^b) + s^b| = \Delta \tag{3.74}$$

all the singular regions in Fig. 4 disappear. Similarly, if

$$\delta^2(p^a - p^b) + s^b = 0 \tag{3.75}$$

all the singular regions (which have the reversed plastic loading) in Fig. 7 disappear. For cases, such as II.2, V.2, V.6 and V.10, there is no trace left by removing the singular region. In others, such as II.3, V.3, V.7 and V.11, the singular region reduces to a single curve which is a plastic characteristic curve. The singular region in the remaining cases either reduces to an unloading boundary or a loading boundary whose initial speed cannot be obtained by a limiting process. The initial speed of these boundaries has to be determined by using eqn (3.18). Similar situations happen in the problems of discontinuous loading of thin-walled circular-cylindrical tubes studied in [25]. In any case, there are exactly four cases for Group II′ and twelve cases for Group V′. All conditions obtained in Group II and V as indicated in Figs. 4 and 7, apply equally well to Group II′ and V′.

## 4. PLANE STRAIN WAVES

### 4.1 *Introduction*

For cylindrically symmetric waves in which a plane strain state exists, $\epsilon_z = 0$. The only non-zero stresses are $\sigma_{rr}$, $\sigma_{\theta\theta}$ and $\sigma_{zz}$. We will use the notations:

$$p = \sigma_{rr}, \qquad q = \sigma_{\theta\theta}, \qquad n = \sigma_{zz} \tag{4.1}$$

The yield function (2.3) for this case becomes

$$f = \frac{1}{3}(p^2 + q^2 + n^2 - pq - qn - np) \tag{4.2}$$

The stress-strain relation, eqn (2.5), can be written as, after using eqns (2.2), (2.6) and noticing that $\dot{\epsilon}_z = 0$ for a plane strain motion,

$$Ev_{,r} = \dot{p} - \nu(\dot{q} + \dot{n}) + \frac{3}{4}\left(\frac{1}{\beta} - 1\right)s_r(s_r\dot{p} + s_\theta\dot{q} + s_z\dot{n})/k^2 \tag{4.3}$$

$$E\frac{v}{r} = \dot{q} - \nu(\dot{p} + \dot{n}) + \frac{3}{4}\left(\frac{1}{\beta} - 1\right)s_\theta(s_r\dot{p} + s_\theta\dot{q} + s_z\dot{n})/k^2 \tag{4.4}$$

$$0 = \dot{n} - \nu(\dot{p} + \dot{q}) + \frac{3}{4}\left\{\frac{1}{\beta} - 1\right\}s_z(s_r\dot{p} + s_\theta\dot{q} + s_z\dot{n})/k^2 \tag{4.5}$$

where

$$s_r = \frac{1}{3}(2p - q - n)$$

$$s_\theta = \frac{1}{3}(2q - n - p) \tag{4.6}$$

$$s_z = \frac{1}{3}(2n - p - q)$$

Equations (2.1), (4.3), (4.4) and (4.5) can be written in the matrix differential equation form, eqn (3.6), with

$$\mathbf{w} = \begin{bmatrix} v \\ p \\ q \\ n \end{bmatrix} \qquad \mathbf{A} = \begin{bmatrix} 1 & 0 & 0 & 0 \\ 0 & * & * & * \\ 0 & * & * & * \\ 0 & * & * & * \end{bmatrix}$$

$$\mathbf{b} = \begin{bmatrix} 0 & -1 & 0 & 0 \\ -1 & 0 & 0 & 0 \\ 0 & 0 & 0 & 0 \\ 0 & 0 & 0 & 0 \end{bmatrix} \qquad \mathbf{F} = \begin{bmatrix} 0 & 1 & -1 & 0 \\ 0 & 0 & 0 & 0 \\ 1 & 0 & 0 & 0 \\ 0 & 0 & 0 & 0 \end{bmatrix} \tag{4.7}$$

where the non-zero elements of A are indicated by * which can be obtained by a direct substitution.

It should be noted here that, with the change of variables:

$$\sigma_1 = (2p - q - n)/\sqrt{(6)}, \quad \sigma_2 = (q - n)/\sqrt{(2)}, \quad \sigma_3 = (p + q + n)/\sqrt{(3)},$$
$$p = (2\sigma_1 + \sqrt{(2)}\sigma_3)/\sqrt{(6)}, \quad q = (-\sigma_1 + \sqrt{(3)}\sigma_2 + \sqrt{(2)}\sigma_3)/\sqrt{(6)},$$
$$n = (-\sigma_1 - \sqrt{(3)}\sigma_2 + \sqrt{(2)}\sigma_3)/\sqrt{(6)}, \tag{4.8}$$

eqn (4.2) can be reduced to

$$f = (\sigma_1^2 + \sigma_2^2)/2, \tag{4.9}$$

In which $\sigma_3$ is absent. $\sigma_3$ is also absent in the following relations:

$$s_r = 2\sigma_1/\sqrt{(6)}, \qquad s_\theta = (-\sigma_1 + \sqrt{(3)}\sigma_2)/\sqrt{(6)}, \qquad s_z = (-\sigma_1 - \sqrt{(3)}\sigma_2)/\sqrt{(6)}. \tag{4.10}$$

The characteristic wave speeds $c$ as defined in eqn (3.8) are $c = 0, 0, \pm c_p$ in the plastic region where

$$c_p = c_1\left\{1 - \frac{2(1-2\nu)(1-\beta)\sigma_1^2}{(1-\nu)\{2(1+\nu)\beta + 3(1-\beta)\}(\sigma_1^2 + \sigma_2^2)}\right\}^{1/2} \tag{4.11}$$

$$c_1 = \left\{\frac{E(1-\nu)}{\rho(1+\nu)(1-2\nu)}\right\}^{1/2} \tag{4.12}$$

In the elastic region, $\beta = 1$ and $c = 0, 0, \pm c_1$.

The left and right eigenvectors as defined in eqn (3.12) are again identical in this case. We have, for $c = c_1$ or $c_p$,

$$\mathbf{r} = \begin{bmatrix} 1 \\ -\rho c \\ -\rho c\psi \\ -\rho c\Phi \end{bmatrix} \tag{4.13}$$

$$\psi = \frac{\nu(1+\nu) + \left(\frac{1}{\beta} - 1\right)\left\{\frac{8\nu - 1}{4} + \frac{(1-2\nu)(p-q)^2}{4k^2}\right\}}{(1-\nu^2) + \left(\frac{1}{\beta} - 1\right)\left\{\frac{1+\nu}{2} + \frac{(1-2\nu)(q-n)^2}{4k^2}\right\}} \tag{4.14}$$

$$\Phi = \frac{\nu(1+\nu) + \left(\frac{1}{\beta} - 1\right)\left\{\frac{8\nu - 1}{4} + \frac{(1-2\nu)(p-n)^2}{4k^2}\right\}}{(1-\nu^2) + \left(\frac{1}{\beta} - 1\right)\left\{\frac{1+\nu}{2} + \frac{(1-2\nu)(q-n)^2}{4k^2}\right\}} \tag{4.15}$$

4.2 *Continuous loading*

The analysis is similar to that of plane stress waves discussed in Section 3.2. It can be shown that Fig. 1 applies also to the plane strain waves provided we replace $c_L$ in Fig. 1 by $c_1$ and define

$$J(\beta^b) = \sqrt{\left(\frac{2}{3}\right)} \frac{1-2\nu}{1-\nu} \sigma_1{}^b (\dot{p}^a - \dot{p}^b) + \dot{f}^b \left\{1 + \left(\frac{1}{\beta^b} - 1\right)\left(\frac{\sigma_1{}^{b^2}}{1-\nu} + \frac{3\sigma_2{}^{b^2}}{1+\nu}\right) \Big/ (4f^b)\right\} \tag{4.16}$$

$c^*$ in Fig. 1 is defined in eqn (3.33).

4.3 *Discontinuous loading*

The stress paths for "pseudo simple waves" (see Section 3.3) for the plane strain waves can be shown to be governed by the following differential equations:

$$\frac{d\sigma_2}{d\sigma_1} = -\frac{3\left(\frac{1}{\beta} - 1\right)\sigma_1\sigma_2/(\sigma_1{}^2 + \sigma_2{}^2)}{2(1+\nu) + 3(\frac{1}{\beta} - 1)\sigma_2{}^2/(\sigma_1{}^2 + \sigma_2{}^2)} \tag{4.17}$$

$$\frac{d\sigma_3}{d\sigma_1} = \frac{1+\nu}{\sqrt{(2)}(1-2\nu)} \frac{2(1+\nu) + 3\left(\frac{1}{\beta} - 1\right)}{2(1+\nu) + 3\left(\frac{1}{\beta} - 1\right)\sigma_2{}^2/(\sigma_1{}^2 + \sigma_2{}^2)} \tag{4.18}$$

These two equations can be shown to be equivalent to

$$\frac{d\sigma_2}{\sigma_2} + \frac{3}{2(1+\nu)}\left(\frac{1}{\beta} - 1\right)\frac{dk}{k} = 0 \tag{4.19}$$

$$d\left\{\frac{\sqrt{(2)}(1-2\nu)}{1+\nu}\sigma_3 - \sigma_1\right\} = -\frac{\sqrt{(2k^2 - \sigma_2{}^2)}}{\sigma_2} d\sigma_2 \tag{4.20}$$

Therefore, instead of the $(p, q, n)$ space, we will use $(\sigma_1, \sigma_2, \sigma_3)$ space to describe the stress paths, Fig. 8. The stress paths are projected on the $(\sigma_1, \sigma_2)$ plane and $(\sigma_1, \sigma_3)$ plane. In the $(\sigma_1, \sigma_2)$ plane, the stress paths are symmetric with respect to the $\sigma_1$ and $\sigma_2$ axes. In the $(\sigma_1, \sigma_3)$ plane, they are symmetric with respect to the origin. Actually, there are two-parameter family of curves in the $(\sigma_1, \sigma_3)$ plane. Only one-parameter family of curves is shown because the other family can be obtained by translating the curves along the $\sigma_3$ axis. From eqn (4.8), the $\sigma_3$ axis makes equal angles with the $p$, $q$, $n$ axes. Moreover, the $\sigma_1$, $\sigma_3$ and $p$ axes are on the same plane. The relations between $(\sigma, \sigma_2, \sigma_3)$ and $(p, q, n)$ coordinates are given by eqn (4.8) and are illustrated graphically in Fig. 8.

4.4 *Propagation of shock waves*

If the discontinuity in the loading at $r = r_0$ is propagated into $r > r_0$ as a shock wave, it can be shown that eqns (3.47), (3.50) and (3.51) remain valid for plane strain waves provided we replace $c_L$ by $c_1$ and define

$$\delta = (1-2\nu)/(1-\nu), \qquad s = \sqrt{(6)}\delta\sigma_1 \tag{4.21}$$

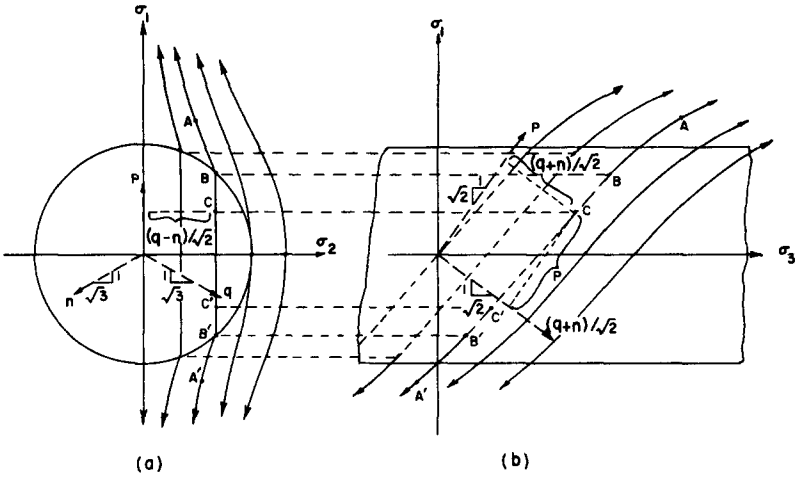


Fig. 8. Stress paths for pseudo-simple waves. (Plane strain and von Mises yield condition.)

4.5 *Cases of discontinuous loadings*

Again, the analysis is similar to that of Section 3.5. In fact the results show that Figs. 3–7 with conditions applied to each case as indicated in the figures remain valid provided we use the definitions of $s$ and $\delta$ given by Eq. (4.21) and redefine $\bar{J}$ by

$$\bar{J}(\beta^b) = \frac{s^a}{3}(\dot{p}^a - \dot{p}^b) + (\sigma_1{}^a\dot{\sigma}_1{}^b + \sigma_2{}^a\dot{\sigma}_2{}^b) + \dot{f}^b\left(\frac{1}{\beta^b} - 1\right)\left(\frac{\sigma_1{}^a\sigma_1{}^b}{1-\nu} + \frac{3\sigma_2{}^a\sigma_2{}^b}{1+\nu}\right)\frac{1}{4f^b}$$

$$- \frac{3E(v^a - v^b)}{\sqrt{(6)}r_0}\left(\frac{\sigma_1{}^a}{1-\nu} - \frac{\sqrt{(3)}\sigma_2{}^a}{1+\nu}\right) \tag{4.22}$$

$$v^a - v^b = -\int_{p^b}^{p^a} \frac{dp}{\rho c} \tag{4.23}$$

Thus, $\Delta$, $Q$, $(p^a - p^b)$, $R^b$, $\bar{Q}$ as defined in eqns (3.58), (3.64), (3.62), (3.70) and (3.73) remain valid if we use the definition of $s$ and $\delta$ given by eqn (4.21). Of course, $c_L$ in Figs. 3–7 has to be replaced by $c_1$.

## 5. LINEAR WORK-HARDENING AND PERFECTLY-PLASTIC SOLIDS

The analysis presented in the previous sections can be modified to include linear work-hardening materials ($\beta$ = constant) and perfectly-plastic solids ($\beta = 0$; $\dot{f}^p = 0$). For the latter material the value of $\lim_{\beta\to 0} \dot{f}^p/\beta$ is obtained from eqns (3.2)–(3.4) for plane stress waves and eqns (4.2)–(4.5) for plane strain waves. The most significant modification concerns the stress-paths for pseudo-simple waves.

5.1 *Plane stress waves*

For linear work-hardening solids the stress paths of Fig. 2 will have the new property that they have the same slope along any radial line passing through the origin. This follows from eqn (3.39) in which $\psi$ is a function only of $(p/q)$. Equation (3.39) can be integrated analytically (see [26]).

For perfectly-plastic solids, the yield surface is invariant and the stress paths coincide with the yield surface. This is seen from eqn (3.14) as $\psi$ becomes identical to the slope of the yield surface at all points. For a valid pseudo-simple wave solution, the state of stress must traverse the yield surface in the direction of decreasing $c_p$. Figure 9 shows the admissible directions for the change of stress state as $c_p$ decreases. From Fig. 9, we see that

$$|p| \le 2k_y \tag{5.1}$$

where $k_y$ is the constant yield stress.

If the values of $(p, q)$ for $t < 0$ correspond to point A, Fig. 9, any discontinuous increase in $p$

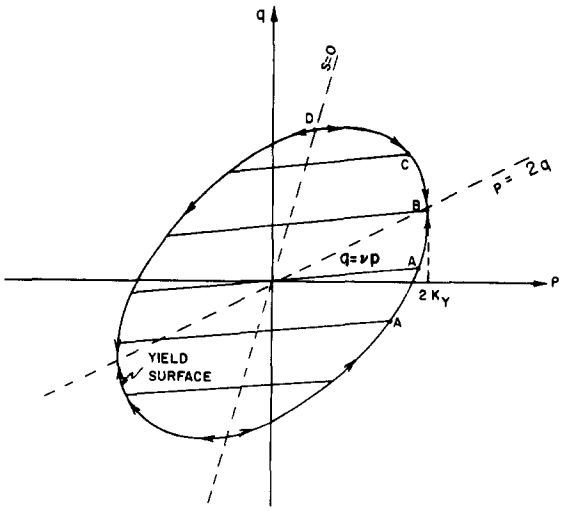


Fig. 9. Stress paths for pseudo-simple waves in perfectly-plastic solids. (Plane stress and von Mises yield condition.)

causes the state of stress to traverse the yield surface toward point B while any discontinuous decrease in $p$ causes an unloading via the line of slope $\nu$ passing through A. A similar situation holds for point C. But if the initial state corresponds to point D, any arbitrary discontinuous change in $p$ results in plastic response. On the other hand, if the initial state corresponds to point B, any change in $p$ has to be a decrease and we can have unloading only.

5.2 *Plane strain waves*

For linear work-hardening solids the stress paths of Fig. 8(a) become similar and the differential equation governing the stress paths can be integrated analytically,[26].

A special case arises when $q = n$, or $\sigma_2 = 0$. This case is of particular interest because it arises when the medium is initially at rest and stress free and is subjected to a discontinuous pressure. From eqn (4.11) we see that $c_p$ is a constant since $\beta$ is a constant and $\sigma_2 = 0$. From Fig. 8(a), we see that the stress path for this case is the line $\sigma_2 = 0$. This is the only case of cylindrical waves in which a part of the discontinuity $(p^a - p^b)$ may propagate, initially at least, as a plastic shock wave across which w is discontinuous. But since it may not be possible to maintain the condition $q = n$ for any length of time, this shock wave may degenerate into weak discontinuity waves in the neighborhood of $r = r_0$.

For perfectly-plastic solids, the yield surface is a circular cylinder of radius $\sqrt{(2)}k_y$, where $k_y$ is the constant yield stress. The stress paths now lie on the surface of this yield surface. Figure 10 shows the projections of these stress paths. The projections of the stress paths on the $\sigma_1 \sim \sigma_2$ plane coincide with the projection of the yield surface. The stress paths in this case constitute a

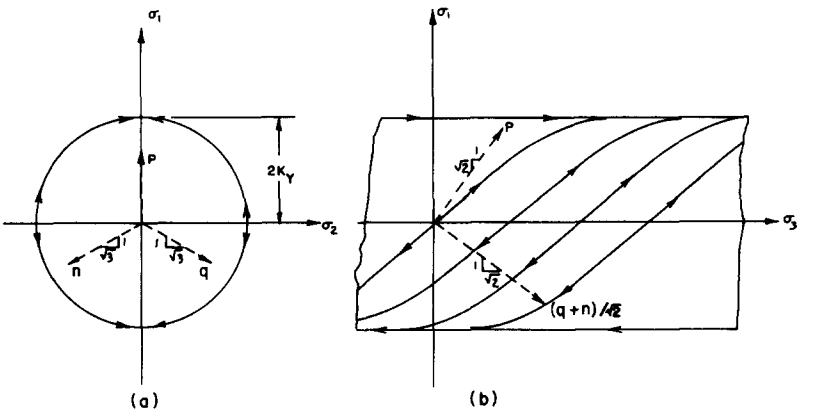


Fig. 10. Stress paths for pseudo-simple waves in perfectly plastic solids. (Plane strain and von Mises yield condition.)

one-parameter family of curves and their projections on the $\sigma_1 \sim \sigma_3$ plane may be obtained by translating any one of them along the $\sigma_3$ axis.

## 6. SOLIDS OBEYING TRESCA YIELD CRITERION

Since we do not know a priori which of the principal stresses are maximum and minimum, we define $f$ as,

$$f = \frac{1}{16}\{|p-q|+|q-n|+|n-p|\}^2 = \frac{1}{16}\{n_1(p-q)+n_2(q-n)+n_3(n-p)\}^2 \tag{6.1}$$

where

$$n_1 = sgn(p-q), \quad n_2 = sgn(q-n), \quad n_3 = sgn(n-p). \tag{6.2}$$

Then Tresca yield criterion is given by

$$f = k^2. \tag{6.3}$$

The quantities $n_1$, $n_2$ and $n_3$ must satisfy one of the following equations depending on the location of $(p, q, n)$ in the stress space:

$$\begin{aligned} &\text{Region I: } n_1n_2 = -n_2n_3 = -n_3n_1 = 1 \\ &\text{Region II: } n_2n_3 = -n_3n_1 = -n_1n_2 = 1 \\ &\text{Region III: } n_3n_1 = -n_1n_2 = -n_2n_3 = 1 \end{aligned} \tag{6.4}$$

Thus we will have three possible cases. For each case, we can derive the basic equations as in Section 2 by replacing $f$ of eqn (2.3$_1$) by that of eqn (6.1). While Fig. 1 holds good for each of the above three cases, we have to derive the conditions governing them. Since this procedure is exactly the same as that of Sections 3.2 and 4.2, we omit these details.

The cases arising due to discontinuous loading can be obtained by an analysis similar to that of Sections 3.3, 3.4 and 3.5. The essential difference is in the pseudo-simple wave solution. Omitting all other details we briefly describe this aspect only.

### 6.1 *Plane stress waves*

Figure 11 shows the schematic diagram of stress paths for pseudo simple waves. Inside the yield surface, the stress paths are lines of slope $\nu$. Outside the yield surface, we divide the stress-space into three regions according to eqn (6.4). The stress paths in region I are lines of slope $\nu$ as those inside the yield surface. The stresses may traverse only in the outward direction

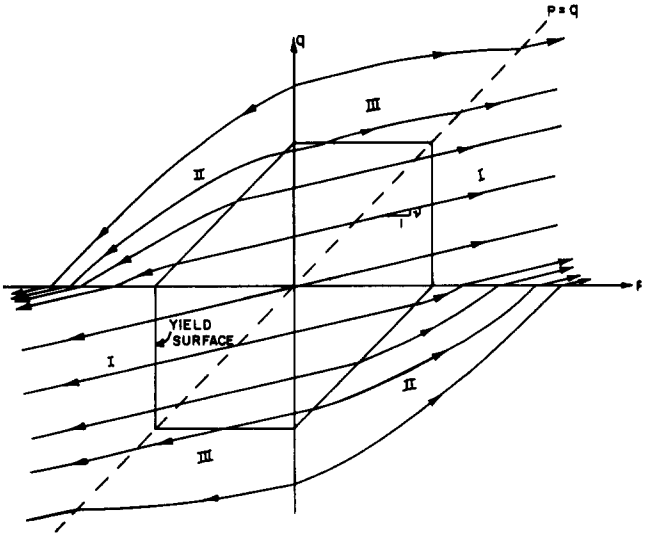


Fig. 11. Stress paths for pseudo-simple waves. (Plane stress and Tresca's yield condition.)

as indicated by the arrows. In region II, the stress paths are curves and their slopes which are always positive, approach $\nu$ as $\beta \to 1$ and 1 as $\beta \to 0$. The stress paths in region III are curves and their slopes which are always positive also approach $\nu$ as $\beta \to 1$ but approach 0 as $\beta \to 0$. It may be noted that the slope of the stress paths may be discontinuous along the lines $p = 0$, $q = 0$ and $p = q$.

### 6.2 *Plane strain waves*

Figure 12 shows the projections of the stress paths on the $\sigma_1 \sim \sigma_2$ and $\sigma_1 \sim \sigma_3$ planes, where $\sigma_1$, $\sigma_2$ and $\sigma_3$ are defined by eqn (4.8). The yield surface in this case is a hexagonal cylinder with its axis coinciding with the $\sigma_3$ axis. Referring to Fig. 12(a), we divide the stress space outside the

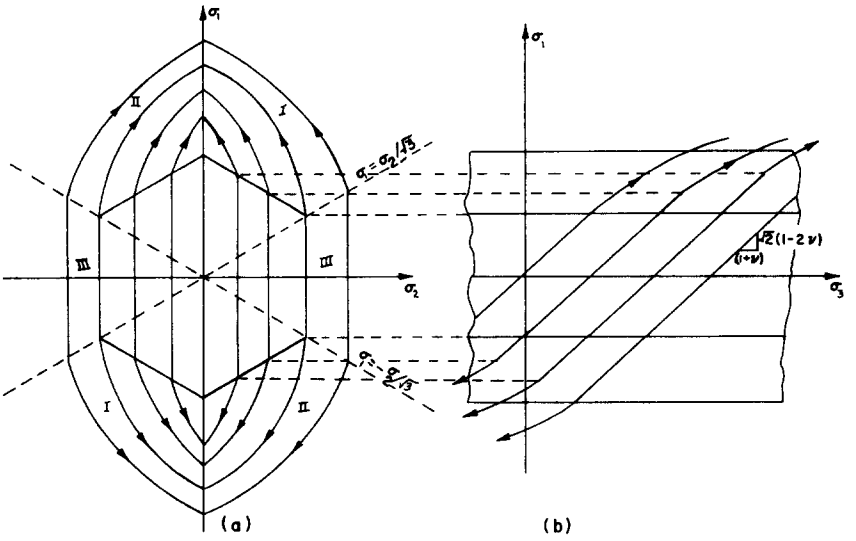


Fig. 12. Stress paths for pseudo-simple waves. (Plane strain and Tresca's yield condition.)

yield surface into regions according to eqns (6.4). In region I, the slopes of the projections of the stress paths on $\sigma_1 \sim \sigma_2$ plane and $\sigma_1 \sim \sigma_3$ plane depend on $\beta$ only. In the $\sigma_1 \sim \sigma_2$ plane, the slope varies from $-\infty$ to $-1/\sqrt{(3)}$ as $\beta$ decreases from 1 to 0. In the $\sigma_1 \sim \sigma_3$ plane it varies from $\sqrt{(2)}(1-2\nu)/(1+\nu)$ for $\beta = 1$, to $(1-2\nu)/2\sqrt{(2)}(1+\nu)$ as $\beta \to 0$. The projections of stress paths in region II are mirror images of region I with respect to the $\sigma_1$ axis. The stress paths in region III are lines, the projections of which are parallel to the $\sigma_1$ axis in the $\sigma_1 \sim \sigma_2$ plane and have the slope of $\sqrt{(2)}(1-2\nu)/(1+\nu)$ in the $\sigma_1 \sim \sigma_3$ plane. Since $c_p = c_1$ in this region, the stress paths in this region are indistinguishable from those inside the yield surface. As in the case of plane stress, the slope of the stress paths may be discontinuous where they intersect the lines $\sigma_1 = \pm\sigma_2/\sqrt{(3)}$.

## CONCLUDING REMARKS

The results presented here enable one to determine exactly what kind of waves one would obtain for a given loading which has some kind of discontinuities. The solutions are exact solutions near the point of discontinuity. Since the theory assumes that the material is rate-independent, the results obtained here do not apply to rate-sensitive materials. This is particularly so in the cases where the discontinuity involves a sudden change in the load applied at the cavity. In the plastic region this implies infinite strain rate, and hence the effect of rate-sensitivity cannot be ignored no matter how small the rate-sensitivity is. In the latter cases, the solutions obtained by the present anslysis can be regarded as an approximate solution in some region near, but not adjacent to, the cavity.

*Acknowledgements*—Portions of this work were carried out while the authors were visiting at Stanford University. The authors are grateful for the warm hospitality and the excellent research environment provided by Professor George Herrmann, Head of the Department of Applied Mechanics. This work is supported by the National Science Foundation Grant GK35163 through the University of Illinois at Chicago Circle.

## REFERENCES


1. A. Kromm, On the propagation of stress waves in circular cylindrical plates. *ZAMM* **28**, 104 (1948).
2. H. J. Plass and B. C. Ellis, Solution of some problems of cylindrical waves in flat elastic plates. *Development in Mechanics* Vol. 2. Pergamon Press, Oxford (1965).
3. P. C. Chou and H. A. Koenig, A unified approach to cylindrical and spherical elastic waves by method of characteristics. *J. Appl. Mech.* **33**, 159 (1966).
4. N. Cristescu, Some observations concerning the propagation of plastic waves in plates (axisymmetric case). (in Russian) *Prikl. Mat. Mech.* **18**, 433 (1955).
5. E. H. Agababian, Stresses in a tube for a suddenly applied load. (in Russian) *Ukr. Mat. Zhur.* **5**, 325 (1953).
6. E. H. Agababian, Dynamic expansion of a hollow cylinder in condition of perfect plasticity, (in Russian) *Ukr. Mat. Zhur.* **7**, 243 (1955).
7. A. P. Bronskii, The velocity of deformation of a hollow cylinder subjected to an internal pressure. (in Russian) *Vest. Moscow University* No. 1, 13 (1956).
8. I. Z. Stepanenko, Expansion of a circular cylindrical tube subjected to a dynamic load, (in Ukranian) *Prik. Mekh.* **3**, 225 (1957).
9. N. Cristescu, Some observations about the case of plane axial-symmetric deformations in the dynamic problem of plasticity (Prandtle-Reuss theory). (in Roumanian), *Com. Acad. Rep. Pop. Rom.* **6**, 19 (1956).
10. R. R. Ensminger and I. M. Fyfe, Constitutive model evaluation using cylindrical stress wave propagation. *J. Mech. Phys. Solids* **14**, 231 (1966).
11. I. M. Fyfe, Plane-stress plastic wave propagation in a dynamically loaded hollow cylinder. In *Mechanical Behavior of Materials under Dynamic Loads* (Edited by U.S. Lindholm). Springer Verlag, N.Y. (1968).
12. R. P. Swift and I. M. Fyfe, Elastic/viscoplastic theory examined using radial cylindrical stress waves. *J. Appl. Mech.* **37**, 1134 (1970).
13. L. E. Malvern, Current Topics in dynamic Plasticity. *Proc. 10th Anniv. Meeting Soc. Engng Sci.* (1973).
14. R. J. Clifton, Plastic waves: theory and experiment. *Mechanics Today* (Edited by S. Nemat-Nasser) Vol. 1, 1972. Pergamon Press, Oxford (1974).
15. J. A. Duffey, Approximate solution of an impulsively loaded long cylinder generated by an elastic-plastic material law. *Acta Mech.* **11**, 45 (1971).
16. P. A. Mehta, Cylindrical and spherical elastoplastic stress waves by a unified direct analysis method. *AIAA Journal* **5**, 2242 (1967).
17. M. G. Srinivasan and T. C. T. Ting, Initiation of spherical elastic-plastic boundaries due to loading at a spherical cavity. *J. Mech. Phys. Solids* **22**, 415 (1974).
18. R. Hill, *The Mathematical Theory of Plasticity*. The Clarendon Press, Oxford (1956).
19. R. J. Clifton, An analysis of combined longitudinal and torsional plastic waves in thin-walled tube. *Proc. 5th U.S. Nat. Cong. of Appl. Mech. ASME*, 465 (1966).
20. T. C. T. Ting, A unified theory on elastic-plastic wave propagation of combined stress. In *Foundations of Plasticity*. (Edited by A. Sawczuk). Noordhoff, New York (1972).
21. E. H. Lee, A boundary value problem in the theory of plastic wave propagation. *Quart. Appl. Math.* **10**, 335 (1953).
22. R. J. Clifton, Elastic-plastic boundary in combined longitudinal and torsional wave propagation. *J. Appl. Mech.* **35**, 782 (1968).
23. T. C. T. Ting, On the initial slope of elastic-plastic boundaries in combined longitudinal and torsional wave propagation. *J. Appl. Mech.* **36**, 203 (1969).
24. T. C. T. Ting, On the initial speed of elastic-plastic boundaries in longitudinal wave propagation in a rod. *J. Appl. Mech.* **38**, 441 (1971).
25. T. C. T. Ting, The initiation of combined stress waves in a thin-walled tube due to impact loadings. *Int. J. Solids Structures* **8**, 269 (1972).
26. T. C. T. Ting, Plastic wave propagation in linearly work-hardening materials. *J. Appl. Mech.* **40**, 1045 (1973).